Journal of Applied Physics

From lab to lamp: Understanding downconverter degradation in LED packages

Cite as: J. Appl. Phys. **132**, 190901 (2022); https://doi.org/10.1063/5.0122735
Submitted: 25 August 2022 • Accepted: 18 October 2022 • Published Online: 15 November 2022

Shruti Hariyani, Jakoah Brgoch, Florencio Garcia-Santamaria, et al.

AIP Publishing

Journal of Applied Physics PERSPECTIVE scitation.org/journal/jap

From lab to lamp: Understanding downconverter degradation in LED packages

Cite as: J. Appl. Phys. **132**, 190901 (2022); doi: 10.1063/5.0122735
Submitted: 25 August 2022 · Accepted: 18 October 2022 ·
Published Online: 15 November 2022

Shruti Hariyani,[1,2] Jakoah Brgoch,[1,2] Florencio Garcia-Santamaria,[3,a)] Srinivas P. Sista,[3,b)] James E. Murphy,[3] and Anant A. Setlur[3,c)]

AFFILIATIONS

[1]Department of Chemistry, University of Houston, Houston, Texas 77204, USA
[2]Texas Center for Superconductivity, University of Houston, Houston, Texas 77204, USA
[3]GE Global Research Center, Niskayuna, New York 12309, USA

[a)]**Present address:** ams-OSRAM, Exeter, NH 03833, USA.
[b)]**Present address:** GE Healthcare, Milwaukee, WI 53219, USA.
[c)]**Author to whom correspondence should be addressed:** setlur@ge.com

ABSTRACT

Downconverters, primarily inorganic phosphors, are critical components in white solid-state LED-based lighting and liquid crystal display backlights. Research efforts have led to a fundamental understanding of a downconverter's absorption, photoluminescence, and efficiency as a function of composition, structure, and processing conditions. However, considerably less work has focused on the reliability of phosphors once they are incorporated into LED packages. Solving these issues is often the final step before the commercialization of new materials, but the significant resources and time required to evaluate and mitigate materials failure are rarely discussed in the literature. In this Perspective, we discuss the need for conducting downconverter reliability testing and the potential of accelerating, screening, and understanding downconverter failure modes. Our focus highlights the mechanisms of failure and discusses how this influences materials selection and the design of different LED packages. We also stress the potential for accelerated reliability testing protocols and note the potential role first-principles calculations and data-driven models could play in establishing the compositional-processing trends for different aspects of downconverter reliability. We close with possible research directions that could improve downconverter reliability and emphasize the importance of assessing a material's (chemical) stability where multiple manufacturing and processing steps can dictate system performance.

I. INTRODUCTION

Phosphor-converted light-emitting diodes (LEDs) have become ubiquitous in lighting and displays due to their form factor, higher energy efficiency, and longer operating lifetime compared to traditional light sources. The U.S. Department of Energy estimates that transitioning to LED lighting technology has saved 185 TW h of site energy, avoided 79×10^6 metric tons of carbon dioxide emissions, and saved consumers ≈$20 billion in 2020.[1,2] Most of these devices produce an energy-efficient white light by downconverting the nearly monochromatic emission from a blue-emitting LED chip to longer wavelengths using transition-metal or rare-earth substituted inorganic phosphors (Table I). In most LED packages, phosphors are mixed in an optically transparent silicone resin and deposited onto the surface of a blue-emitting (InGa)N LED chip. The choice of phosphor is dictated by the application with most LED-based light bulbs using a phosphor mixture of yellow-emitting $Y_3Al_5O_{12}:Ce^{3+}$ and a red-emitting phosphor, such as $CaAlSiN_3:Eu^{2+}$. LEDs for liquid crystal display (LCD) backlights use a similar phosphor-converted approach but incorporate phosphors with narrower emission bands, such as green-emitting β-SiAlON:Eu^{2+} and red-emitting $K_2SiF_6:Mn^{4+}$. In an effort to continually advance the capability of LED-based lighting and displays, research groups around the world are utilizing exploratory synthesis,[3] the creation of solid solutions,[4,5] and data-driven methods[6,7] to identify new, high efficiency phosphors that can be used in phosphor blends with improved color rendering (for lighting) or a wider gamut (for displays).

Although the potential for LED applications has reinvigorated phosphor research across many different materials systems,

TABLE I. Phosphors used in typical, commercial LED packages.

Phosphor	Emission color	FWHM of the emission band	Current usage
$Y_3Al_5O_{12}:Ce^{3+}$ ($YAG:Ce^{3+}$)	Yellow	>100 nm	Most general illumination white LEDs Lower-cost LCD backlights
β-$SiAlON:Eu^{2+}$	Green	~50 nm	Higher color quality LCD backlights
$(Sr,Ca)AlSiN_3:Eu^{2+}$ (SCASN)	Red to deep-red	>75 nm	General illumination for indoor applications Higher color quality LCD backlights
$(Ca,Sr,Ba)_2Si_5N_8:Eu^{2+}$	Orange to red	>75 nm	General illumination for indoor applications
$SrLiAl_3N_4:Eu^{2+}$ ($SLA:Eu^{2+}$)	Deep-red	50 nm	High color rendering general illumination
$K_2SiF_6:Mn^{4+}$ ($KSF:Mn^{4+}$)	Red	Line-emitter, 30 nm Gaussian equivalent	Higher color quality LCD backlights High color rendering general illumination

meeting the basic application requirements, such as ideal emission color, strong absorption of LED radiation, and high quantum efficiency (QE), does not automatically lead to phosphor commercialization. One factor often not considered in early-stage research is material reliability, defined as the ability of a system (the LED package) or a component (the phosphor, silicone, LED, etc.) to perform its function under specific operating conditions for a required period of time.[8] Reliability is often quantified as the mean time to failure, typically defined as either a loss in LED efficacy or a shift in LED color with various standards, testing protocols, and requirements based upon different applications.[8–10] In many cases, failure modes can be from long-term phosphor degradation in LED packages and systems under operating conditions. Thus, it is important to uncover the mechanisms of degradation in phosphors (and the package, in general) and establish methods to mitigate failure. As with many materials systems, achieving phosphor reliability in LED packages is multifaceted: phosphors must withstand degradation from high-intensity blue light excitation and heat generated by the LED (Table II).[11] The phosphors should also resist degradation from ambient moisture, solvents, and the processing equipment used in LED package production. Finally, the entire system must be unaffected by harsh climates, such as high ambient temperatures, solar radiation, and dirt accumulation.[12] The goal of developing LED packages and systems with desired product lifespans relies on robustness to relevant stimuli and environments in different applications.

Unfortunately, material stability with respect to all of these metrics is often difficult to predict and costly to test, especially at early stages of materials development. Identifying and mitigating reliability and stability issues can be a significant part of the development cycle for a new material or system design. Even in the relatively mature LED industry, the primary path toward addressing downconverter reliability is often through extensive iterative testing and an *ad hoc* understanding of individual reliability issues for a specific material. Longer development cycles with associated costs to address reliability concerns make it more challenging to incorporate new materials or designs even when they have potential technical advantages, such as better emission color or higher initial quantum efficiencies. In this Perspective, we discuss designing experimental and theoretical frameworks to improve the ability for screening, quantifying, and developing a fundamental understanding of downconverter reliability. Specifically, we discuss various paths for downconverter degradation in LED packages and systems as a function of composition and/or processing, the potential for accelerated reliability screening and testing, and the development of first-principles and data-driven trends for different failure modes.

TABLE II. LED packages and systems.

System/package	Incident light flux	Downconverter temperature	Matrix for phosphor	Examples of phosphor-package integration issues	Median particle size
Laser excited phosphor for small spot sizes	>100 W/cm^2	>100 °C	State of the art are monolithic phosphor ceramic converters		
Higher power LED package (>0.5 W)	50–100 W/cm^2	>100 °C	Permeable silicones	Metal tarnishing	10–25 μm
Low/medium-power LED package (0.05–0.5 W)	10–80 W/cm^2	50–125 °C	Permeable silicones	Metal tarnishing	10–25 μm
Remote downconverters	<1 W/cm^2	<75 °C	Polymer	Barrier layers	5–25 μm for phosphors; QD downconverters have much smaller individual particle sizes
Micro (<100 μm) LED systems	<2 W/cm^2	<60 °C	Not standardized	Integration into inks	<3 μm

Extending the experimental and theoretical framework toward other materials systems is also discussed.

II. THE RELIABILITY REQUIREMENTS OF VARIOUS LED PACKAGES

LED packages using phosphor/silicone mixtures directly deposited onto LED chips (Fig. 1) are the dominant platform for white light production in lighting and displays. The median phosphor particle sizes in these devices usually range from 5 to 25 μm depending on the phosphor composition and specific packaging needs. This technology has matured significantly over the past 25 years, and LED packages routinely meet color and light output stability requirements for greater than 25 000 h. The relative standardization of these packages and their performance means that the flow-up from LED to system reliability is reasonably understood.

The workhorse yellow phosphor for most of these LEDs, $Y_3Al_5O_{12}:Ce^{3+}$ (YAG:Ce^{3+}) and its compositional variations, has the advantage of stability under high-intensity blue light excitation and inherent chemical durability. Improving LED color quality for LCD backlights and general illumination applications has also led to extensive phosphor research and development toward new compositions and materials.[13–17] These efforts, combined with other work studying Ce^{3+}/Eu^{2+} luminescence,[18–24] have given fundamental and practical insights toward host/activator interactions that control phosphor absorption, emission color, and efficiency at relevant operating temperatures. Currently, few phosphor families are extensively used in commercial LED packages (Table I), and each of these materials has undergone extensive development to optimize initial brightness and durability. However, apart from emission color metrics guiding research and development toward phosphors with narrower emission spectra,[25] fundamental guidelines toward whether or not a new phosphor can match or surpass the performance of current state-of-the-art phosphors are extremely limited. This uncertainty is magnified for reliability metrics since there are even fewer fundamental guidelines for how a phosphor will respond to high-intensity blue light, elevated temperature, ambient humidity, and their combinations.

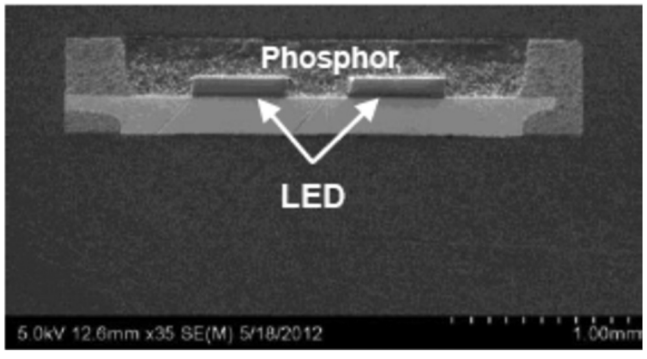

FIG. 1. Cross-sectional SEM micrograph of a typical medium-power LED package where a phosphor/silicone mixture is directly deposited onto an LED chip.

Beyond typical LED packages, how different downconversion materials can fit into system reliability metrics becomes murkier. LED industry maturation with lower LED chip costs has led to LED-based systems with a variety of designs and form factors depending upon specific lighting and display requirements (Table II). LED systems ranging from high-intensity, point source-like light distributions (such those used for automotive headlights) to diffuse panel light sources will have different downconverters and packaging requirements. Diffuse light sources generally have less stringent downconverter reliability requirements with respect to temperature and incident light flux. The exact standards for an LED or phosphor in a specific application are often listed in reports written by technical organizations. For example, the standards for LED packages used in automotive applications are reported by the International Electrotechnical Commission or SAE International.[26,27] Unfortunately, these reports are difficult for academics to obtain since they are not open-access. Moreover, the stability requirements that are listed in these reports are not generalizable across all fields of solid-state lighting and displays, making it difficult to know which properties and environments to target during preliminary reliability experimentation.

The reliability for components in LED packages and systems is also continually evolving. One recent example of how changes in LED system designs alter potential downconverter selection is the use of "remote" downconverter parts with relatively low incident light fluxes and temperatures. The use of remote downconverters has enabled the use of semiconductor quantum dot (QD) downconverters that otherwise have difficulty meeting reliability requirements in typical LED packages. New form factors, such as remote downconverters, introduce potential degradation modes through compatibility and stability concerns between downconverting materials and the variety of solvents, dispersants, and polymer matrices used in these downconversion components. In addition, processing parameters for different form factors may require smaller phosphor/downconverter particle sizes, potentially creating new reliability concerns for materials that would otherwise be completely stable when used in typical LED packages.[28]

III. DOWNCONVERTER DEGRADATION THROUGH APPLIED EXTERNAL STIMULI

A. Environmental degradation

Lighting and display systems using LEDs are usually not hermetically encapsulated, leading to ambient humidity exposure during operation. Hermetic encapsulation is possible, but the additional materials and processes will increase materials and production costs. Therefore, any degradation mode involving oxidation or hydrolysis should be considered for LED package and system reliability. Exposure to high temperatures can lead to irreversible losses in light output caused by a combination of heat-induced effects, including lower crystallinity,[29] the formation of impurities or amorphous surfaces,[30] or oxidation of the activator ion upon contact with adsorbed oxygen.[31] The combination of high temperature (Table II) and water in the atmosphere also accelerates oxidation issues as well as introduction issues for hydrolytic stability. The impacts are present for a variety of different hosts and activator ions. For instance, sulfide phosphor hosts can degrade under

ambient conditions depending upon their synthesis and processing.[32] Similarly, in the red-emitting $Sr_2Si_5N_8:Eu^{2+}$ phosphor, there are various pathways that led to significant emission intensity loss after exposure to 300 °C in air as an accelerated test. As shown in Fig. 2(a), the relative intensity of the most intense (122) diffraction peak of $Sr_2Si_5N_8:Eu^{2+}$ decreases as a function of temperature, which suggests decreased crystallinity. High resolution transmission electron microscopy (HRTEM) revealed a crystalline surface prior to heating [Fig. 2(b)], but an amorphous layer forms after heating [Fig. 2(c)]. Finally, a combination of x-ray absorption near edge spectroscopy (XANES) and electron spectroscopy for chemical analysis (ESCA) measurements, shown in Figs. 2(d) and 2(e), revealed the oxidation of Eu^{2+} to Eu^{3+} and an increase in oxygen adsorbed onto the surface of the material, respectively. In this material, there have been efforts in improving $Sr_2Si_5N_8:Eu^{2+}$ stability by coating phosphor particles with Al_2O_3 using atomic layer deposition (ALD).[33] Improved phosphor stability through particle coatings supports the basic mechanism of phosphor degradation through surface reactions and oxidation.

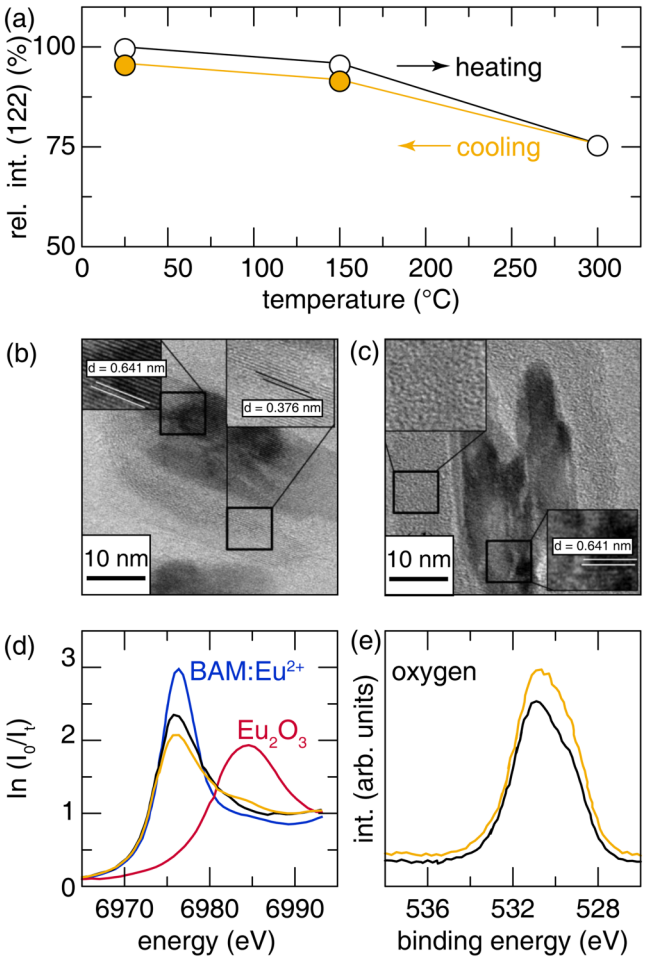

FIG. 2. (a) The relative intensity of the (122) diffraction peak of $Sr_{1.9}Eu_{0.01}Si_5N_8$ upon heating (black) and cooling (yellow). High resolution transmission electron micrographs of $Sr_{1.9}Eu_{0.1}Si_5N_8$ (b) before and (c) after the heat treatment at 300 °C shows the presence of an amorphous phase after heating. (d) The Eu L_3-edge XANES spectra of $Sr_{1.9}Eu_{0.1}Si_5N_8$ before (black) and after (yellow) the heat treatment. The Eu^{2+} reference was commercial $BaMgAl_{10}O_{17}:Eu^{2+}$ (blue, $BAM:Eu^{2+}$) and the Eu^{3+} reference was Eu_2O_3 (red). (e) Wide scan electron spectroscopy for chemical analysis of oxygen in $Sr_{1.9}Eu_{0.1}Si_5N_8$ before (black) and after (yellow) heat treatment. Data are taken with permission from Yeh *et al.*, J. Am. Chem. Soc. **134**(34), 14108–14117 (2012). Copyright 2012 American Chemical Society.

The GE authors of this work also have had a direct experience in working through oxidative and hydrolysis damage modes in the $K_2SiF_6:Mn^{4+}$ phosphor used in LCD backlights and high color rendering lighting.[34,35] In many traditional LED phosphors, oxidative damage often results in reduced phosphor intensity in the LED system/package through losses in phosphor absorption and scattering effects, but these effects are comparatively small vs those that create new absorption centers, such as hydrolysis of the $(MnF_6)^{2-}$ groups to reduced Mn oxides and hydroxides (Fig. 3). If this phosphor "browning" occurred in a LED package/system, there are rapid and unacceptable lumen losses. Therefore, time and effort have been spent developing processing methods and particle coating techniques to reduce the concentration of $(MnF_6)^{2-}$ groups on the particle surface.[34,35] Alternately, other groups have determined that residual impurities in $K_2SiF_6:Mn^{4+}$, such as KHF_2, can adsorb water leading to additional hydrolysis damage[36] vs that of a purer phosphor. Similar to the work on $Sr_2Si_5N_8:Eu^{2+}$, ALD methods have also been applied to fluoride phosphors to improve their chemical stability.[33,37,38] Given the potential flexibility of these methods to improve phosphor chemical stability, additional research in sample purification and particle coating could be helpful across a wide range of materials. The variety of potential reaction paths (and solutions) to hydrolysis and oxidation damage implies that numerous materials and processes may need to be tested and cycled before an appropriate surface chemistry is identified, independent of whether sulfide, nitride, or fluoride materials are being studied.

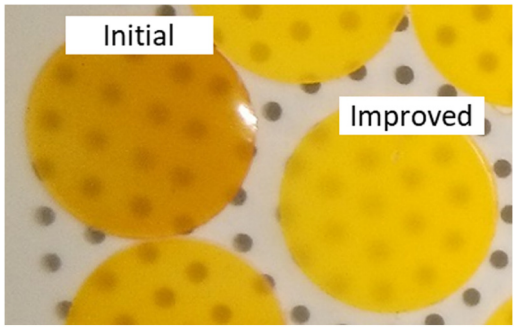

FIG. 3. Photograph of silicone disks containing different $K_2SiF_6:Mn^{4+}$ phosphors after exposure to 85 °C/85%RH for ~100 h. Modifications in phosphor processing lead to significant improvements in hydrolytic stability as noted through the absence of darkening in the disk.

Compared to the testing and optimization of phosphor materials in later stages of development, early-stage materials discovery often has limited access to equipment, such as accelerated aging chambers, that can directly correspond to how a phosphor responds to temperature and humidity. Since chemical stability cannot be ignored when reporting new materials, researchers have turned to more accessible methods to test reliability as part of evaluating new materials. For example, to understand the hydrolysis resistance of $Na_2MgPO_4F:Eu^{2+}$ without using a humidity chamber, the phosphor was submerged in water and agitated using a stir bar for 21 days. Every 7 days, the average crystal structure, the emission spectrum, and QE were measured. This methodology allowed a rudimentary but informative examination of the phosphor's physical and optical response upon contact with water. $Na_2MgPO_4F:Eu^{2+}$ surprisingly showed no change in the x-ray diffractograms, position and shape of the emission band, and the QE even after 21 days in water, indicating that this material is, at this initial testing stage, robust.[39] Conversely, applying this same methodology to the $NaBaB_9O_{15}:Eu^{2+}$ phosphor showed that the material begins to decompose after only 15h in water, revealing inherent instabilities.[40] Some caveats are necessary to draw comparisons between humidity and direct water exposure, such as dissolution and common-ion effects that are not likely to occur in humidity tests. However, straightforward experiments, such as these, are still valuable for learning about material properties and generating data across a broader range of materials.

Materials with smaller particle sizes and a higher surface area will also have higher probabilities for oxidative damage with an extreme case for downconverting films containing semiconducting quantum dots where barrier films are needed for protection from both water and oxygen. Similar barrier films are not required for median particle sizes of ~1 μm for the phosphors listed in Table I, but exploring the limits of this assumption even for "stable" phosphors, such as $YAG:Ce^{3+}$, is another direction for future work.[28]

B. Degradation under high-intensity light excitation

Incident light intensities in traditional LED packages (Table II) are orders of magnitude higher than most spectrophotometer measurements conducted to initially evaluate downconverter performance. High light intensities are known to lead to saturation effects, a sub-linear response to excitation intensity,[41,42] and they can also induce permanent losses in downconverter quantum efficiency (QE) (Fig. 4). Losses in downconverter quantum efficiency under blue light excitation from photo-oxidation and other bleaching processes have been reasonably well documented in quantum dots[43] with some mitigation of these losses through appropriate composition gradients and shell designs.[42] However, in micrometer-sized inorganic phosphors, the current understanding of photo-induced damage mechanisms is more limited. Our observations have been that photo-damaged phosphors have faster decay times, indicating that new non-radiative traps have been created under high-intensity excitation [Fig. 5(a)]. While there is a linear correlation between decay time and intensity loss, the reduction in decay time does not have a one-to-one correlation to lumen losses. This could be due to additional loss mechanisms for this phosphor or experimental artifacts in the decay time measurement. One possible experimental artifact is that the decay profile is measured from the top of the LED package down; therefore, phosphor particles sampled in the decay time measurement are not at the LED chip surface where light intensities are the highest. This observation leads to a notional hypothesis that combining activator redox chemistry with the formation of thermally activated color centers causes quantum efficiency (QE) losses [Fig. 5(b)], but these hypotheses have not been extensively studied experimentally or theoretically. Unlike environmental damage (where barrier coatings reduce damage), research and development pathways toward fixing these reliability issues often do not have clear guidance on modifying composition and synthesis parameters. This forces iterative cycling between materials synthesis and processing optimization with reliability testing giving time, effort, cost, and uncertainty on whether or not these efforts will yield a successful development cycle.

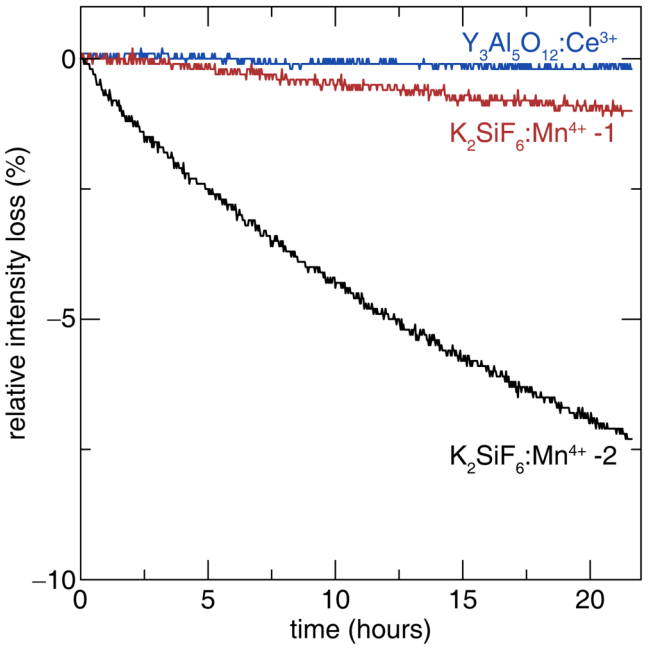

FIG. 4. Comparison of phosphor stability under 80 W/cm^2 laser irradiation for a commercial $Y_3Al_5O_{12}:Ce^{3+}$ phosphor and two different $K_2SiF_6:Mn^{4+}$ phosphors synthesized and processed under different conditions.

C. Chemical reactions with water, solvents, inks, polymers matrices

Phosphors and other downconverters can also have reliability and handling issues with materials, solvents, and processing equipment used in LED packages/systems and their manufacturing. One early example in the LED industry was reactions between sulfide phosphors and package/LED metallization, leading to metal tarnishing and lumen losses. In other cases, these reactions can be classified as hydrolysis reactions, making damage pathways (and mitigations) related to moisture-induced modes, as discussed in Sec. III A. Typical silicone LED encapsulants and their curing agents do not significantly react with the phosphors listed in

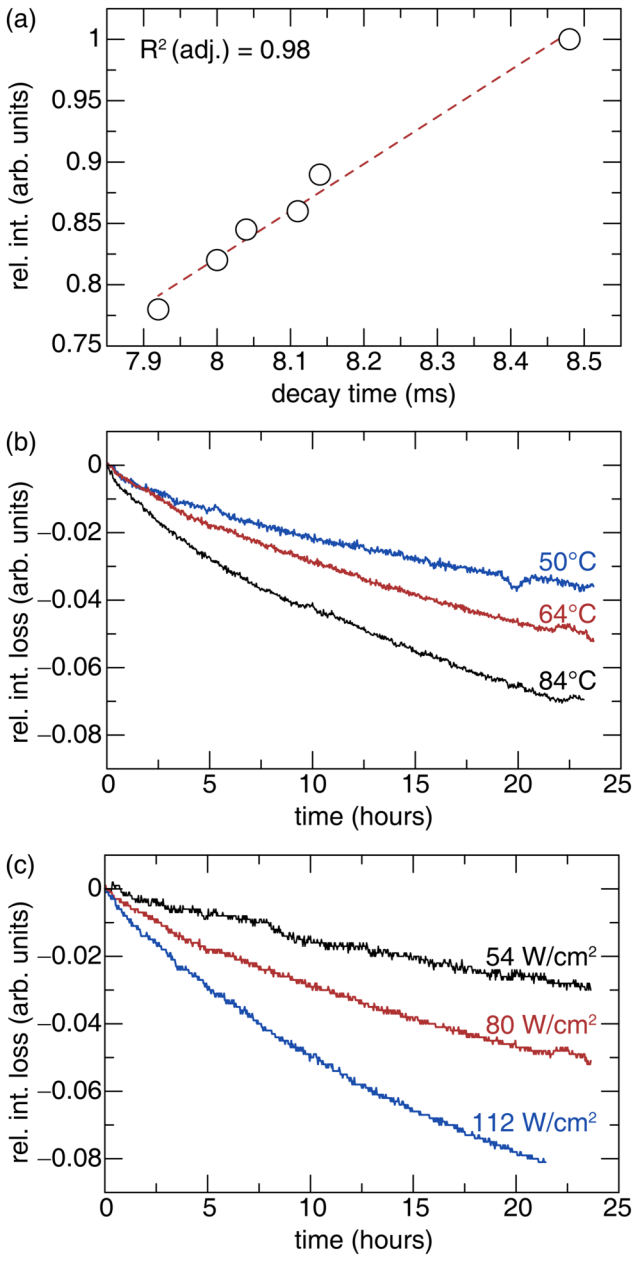

FIG. 5. (a) Correlation between $K_2SiF_6:Mn^{4+}$ relative intensity and $K_2SiF_6:Mn^{4+}$ 1/e decay time for LEDs that contain only $K_2SiF_6:Mn^{4+}$ and were driven under different operating conditions for ~2000 h. The data point at the top right of the figure is from a $K_2SiF_6:Mn^{4+}$ -containing control LED that was stored under dry N_2 at ambient room temperature. The drawn line is from a least-squares linear regression fit. These decay time measurements sample the top surface of the LED. (b) Phosphor intensity loss vs time (~80 W/cm^2 incident laser flux) for a $K_2SiF_6:Mn^{4+}$ sample at different phosphor temperatures. (c) Phosphor intensity loss vs time for a $K_2SiF_6:Mn^{4+}$ sample ($T_{phosphor}$~65 °C) irradiated at different incident laser fluxes. The average phosphor temperature in these experiments using laser excitation was independently calibrated using the emission peak position of $K_2SiF_6:Mn^{4+}$ during measurement.[46]

Table I. Fluoride-based phosphors, such as $K_2SiF_6:Mn^{4+}$, can require extra care in processing to minimize and eliminate any reactive fluoride impurities that may adversely react with the Si–O siloxane bonds in silicone encapsulants. In addition, our observations have been that any improvements in phosphor stability from silicone encapsulation are within experimental errors in either laboratory or LED measurements. Other possible issues are changes in silicone/encapsulant mechanical properties, either from chemical reactions/binding with phosphor surfaces and/or the addition of brittle ceramic particles into a silicone matrix.[44] Higher elastic moduli for a phosphor/silicone composite could enhance brittle fracture due to thermal cycling.

As LED systems are evolving toward smaller LED chip sizes and micro-LED arrays, there is the potential need for printable downconverting layers that can be directly deposited on micro-LED arrays. The requirements to meet downconversion efficiency, reliability, and printability provide multiple challenges for phosphor development. There are issues with the stability of phosphor dispersions in printable and curable inks that depend upon phosphor particle size distributions and surface chemistry. Some of these issues are addressable through traditional colloid/dispersion chemistry, where dispersion stability is maximized when using small, unagglomerated particles. However, any interactions between phosphor particle surfaces and inks that could affect curing characteristics are purely speculative at this time. Since most LED phosphor dopants (Ce^{3+}, Eu^{2+}, Mn^{4+}) could act as oxidation (Mn^{4+}) or reduction (Ce^{3+}/Eu^{2+}) agents, higher surface area phosphor particles could have effects on curing characteristics depending on the specific polymer curing mechanism. Additionally, optimized ink formulations are highly specific to the printing method and architecture of the micro-LED array. Parameters, such as phosphor particle size and percent loading, dispersion stability/zeta potential, and rheological properties (surface tension, contact angle, and viscosity), must be optimized to ensure printability. Several methods, including photolithographic, screen printing, electro-deposition, and digital ink jet printing, may be employed to deposit the phosphor pattern depending on the required resolution/pixel density of the array, and new printing methods are being developed that will inevitably allow phosphor converted micro-LED arrays to proliferate.[45] Since phosphor printing for micro-LED arrays is a nascent technology, the potential issues raised here are speculative but are a potential avenue for future research and analysis.

IV. PROTOCOLS FOR RELIABILITY TESTING AND RELIABILITY EVALUATION

A. Accelerated and higher throughput testing protocols

It is straightforward to envision how higher temperature [Fig. 5(b)], light intensity [Fig. 5(c)], or relative humidity can accelerate downconverter damage and degradation. However, the magnitude of these acceleration factors is experimentally derived, and the analysis is often phenomenological without a deeper understanding of the underlying physics. In our example of the $K_2SiF_6:Mn^{4+}$ phosphor, the super-linear behavior of the QE loss vs incident flux [Fig. 5(c)] gives an indication that a two-photon process is part of the damage mechanism, and the QE loss vs temperature

at a fixed incident flux gives an apparent activation energy of ~0.2 eV [Fig. 5(b)]. However, we can only speculate about the relevant electronic states participating in this two-photon process and the transport/kinetics causing the creation of quenching centers, making paths toward improvement less clear.

When downconverter reliability issues occur, it is necessary to screen through composition and processing iterations in accelerated testing. Understanding acceleration factors is one step in reducing development cycle times, but higher throughput screening methods also can aid in this regard. Prior high-throughput efforts in phosphor development were usually focused on identifying new compositions that could meet brightness or color metrics[47] (Fig. 6); therefore, switching high-throughput screening goals toward reliability will involve changing how these materials are synthesized, processed, and measured. Improvements in automation and computing power can help reduce standard errors in measurements, but generally, total sample and measurement variability is high, making statistically significant assessments of some aspects of downconverter reliability difficult (Fig. 5). Nevertheless, as LED form factors evolve with the variety of binders and solvents that interact with downconverting materials, high-throughput screening methods could become helpful to test chemical stability and durability at different temperatures and conditions, as in prior work for polymer coating weatherability.[48]

B. Extension of laboratory tests toward LED package and system performance

The description for degradation modes given above is simplified in that each way is discussed independently. In actual LED packages and systems, it is evident that various combinations of these modes can occur, and the impact of different damage modes can be time-consuming even before taking appropriate mitigation steps. Even with maps of damage kinetics vs temperature, humidity, light fluxes, etc., reliability in actual packages and systems can be considerably worse than what might be predicted from laboratory tests for a single damage mode. One example from our testing is that any QE losses from hydrolysis-based phosphor darkening at any stage of LED packaging or operation will give higher phosphor temperatures. Higher phosphor temperatures accelerate hydrolysis reactions and light-induced phosphor QE losses (Fig. 5), leading to a feedback loop between phosphor QE and temperature with eventual catastrophic materials failure.

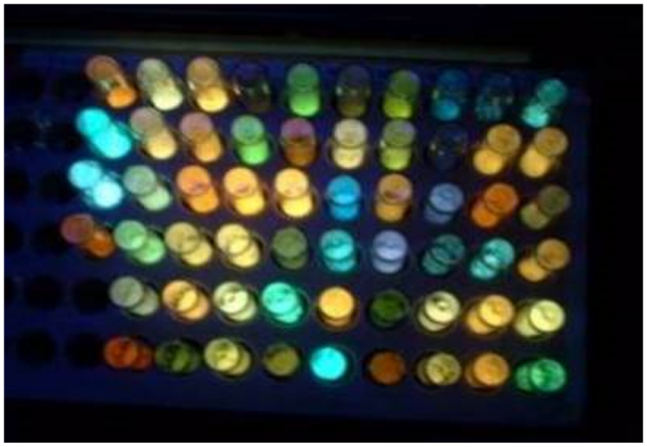

FIG. 6. Image of a combinational phosphor well-plate.

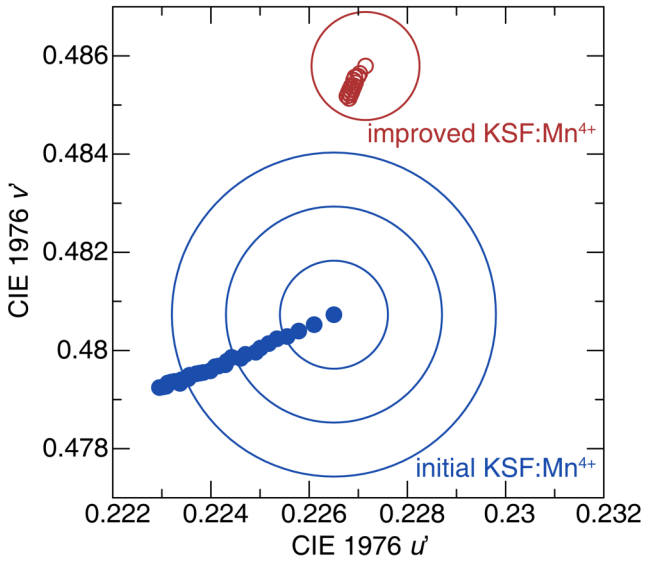

FIG. 7. Color point of ~4000 K LED packages over time with accelerated testing of a 3030 packaged 2-chip LED containing a blend of $Y_3Al_5O_{12}:Ce^{3+}$ and $K_2SiF_6:Mn^{4+}$ (KSF) phosphors dispersed in silicone. Each circle in the figure denotes 1 MacAdam step, and the total test time was ~4000 h.

Our experience with the commercialization of the $K_2SiF_6:Mn^{4+}$ phosphor had initial reliability issues: accelerated testing of packages for general lighting applications had a color shift over time, extrapolating to >4 MacAdam step color shifts in <10 000 h of typical operation (Fig. 7) but without significant lumen losses (<2% under test duration). Since the $K_2SiF_6:Mn^{4+}$ phosphor can undergo both hydrolysis (Fig. 3) and light-based damage (Fig. 5), assigning root causes and relative weights to this color shift was not initially clear. However, combining spectroscopic assessments of phosphors damaged by light (Fig. 5) vs those damaged by hydrolysis along with LED reliability metrics allowed us to appropriately assign a stronger weight to light-based damage for these specific reliability issues. These damage modes have been minimized by implementing improvements in phosphor composition, synthesis, and processing (Fig. 7).[49,50]

C. Materials evaluation and data for understanding and predicting reliability in LED packages

The development of phosphors with improved reliability requires a variety of phosphor and materials characterization techniques to measure and understand reliability under different conditions (Tables III and IV). Phosphor evaluation starts with accurate measurements of powder quantum efficiencies; we suggest that internal quantum efficiencies (IQEs) greater than 70% (at a

TABLE III. Powder-level laboratory measurements to aid in phosphor reliability assessment.

Measurement	Phosphor damage mode	Possible parameters for testing
Water immersion	Hydrolysis during LED packaging and cutting in manufacturing	Immersion in DI H_2O for >24 h at room temperature; sufficient volume of H_2O to reduce likelihood of common-ion effects in dissolution
Phosphor stability in air and controlled humidity environments	Phosphor oxidation and/or hydrolysis	Testing from 60 to 200 °C in ambient humidity for 500 h; testing at 60 °C/90%RH or 85 °C/85%RH for greater than 500 h
Irradiation of phosphor powders or phosphor/encapsulant composites at high incident fluxes	Light-induced damage, photobleaching, color-center formation	Irradiation by blue (435–465 nm) or near-UV (395–415 nm) radiation at incident intensities 1–100 W/cm^2 for 24–1000 h depending upon whether testing is accelerated or to match LED package intensities
Mechanical properties of phosphor/encapsulant composites	Cracking of phosphor/encapsulant composites	Loading of phosphor particles from 1 to 20 vol. %; thermal expansion using dilatometry, elastic modulus measurements from 25 to 250 °C

minimum) are required to start evaluating or understanding inherent reliability issues. If IQEs are much lower than this value, there are too many mitigating factors due to sub-optimal synthesis methods that can obscure "inherent" reliability issues.[36] After this, there are measurements that can be made in LED packages vs materials characterization analysis of LED powders (Tables III and IV). While measurements in LED packages are directly relevant to reliability issues, a mechanistic understanding of degradation modes may require a correlation between these characterization measurements (Table IV), suitable laboratory proxies for damage modes in LED packages (Table III), and LED package data.

V. THE FUTURE OF MATERIALS STABILITY TESTING

A. Using experimental data for machine learning models

Iterative testing of reliability, while successful, is time-intensive and requires continual monitoring with no guarantee of a successful development cycle. Instead, the extensive amount of data collected from these experiments can be used to train machine learning models to extrapolate trends in degradation, guide optimization, and rapidly identify appropriate robust materials. We are not aware of any examples of these methods in the phosphor literature. However, some techniques have been applied in other functional inorganic materials systems.[51] For example, this approach has successfully predicted the capacity and remaining useful life of Li-ion batteries. In the work by Lee and co-workers, electrochemical impedance spectroscopy (EIS) was utilized to obtain the impedance over a range of frequencies by measuring the resulting current upon an applied voltage perturbation.[52] EIS was chosen since the spectra contain information on materials properties, interfacial phenomena, and electrochemical reactions that directly relate to batteries' potential degradation mechanisms.[53] An experimental dataset was constructed by applying a continuous charge–discharge cycle on commercial coin cells in climate chambers where EIS and loss in capacity were measured at alternating charging/discharging cycles. Over 20 000 EIS spectra were

TABLE IV. Potential powder phosphor measurements after laboratory tests, possible correlation to damage modes, and potential for measurement in LED packages.

Phosphor measurement	Potential correlation to LED reliability issues	Possible measurement in LED packages?
Quantum efficiency	General loss in either lumens or color shift	No
Diffuse reflectance	Phosphor photobleaching, creation of new absorption centers	Indirectly through measurement of relative color differences after packaging and/or testing
Decay profile under pulsed excitation	Creation of new quenching centers within the interior of phosphor particles	Yes, possibly limited to the top surface of phosphor further away from the LED emitting surface
IR absorption/reflectance	Detection of hydrolysis products, changes in dopant oxidation states	Perhaps, would need to subtract the encapsulant matrix
XPS of phosphor surfaces	Measurement of surface species related to hydrolytic/oxidative stability	No
X-ray diffraction	Detection of crystalline hydrolysis products, new phase formation	Yes, limited by sensitivity
X-ray absorption spectra	Changes in dopant oxidation states	No
Transmission electron microscopy	Measurement of surface species/morphology related to hydrolytic/oxidative stability	No

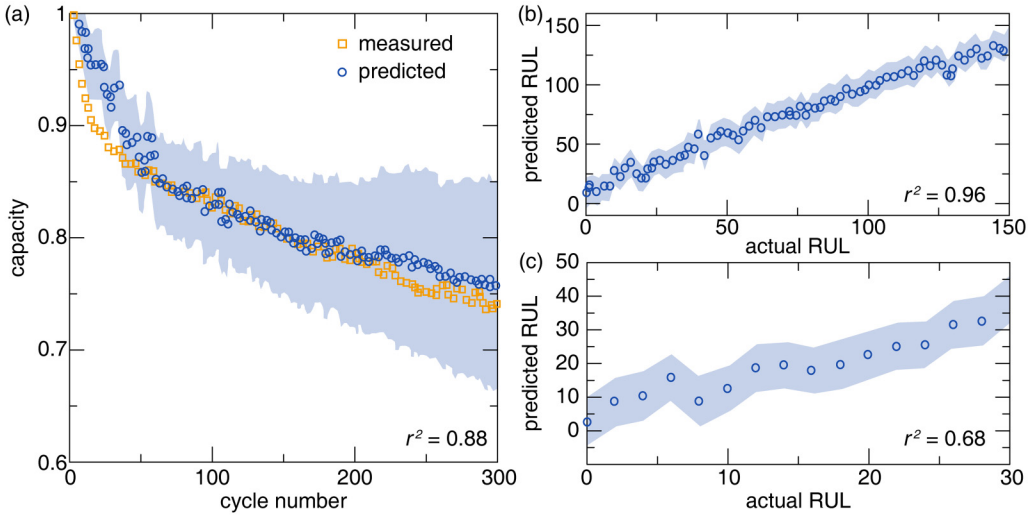

FIG. 8. (a) Measured (yellow square) and predicted (blue circle) of the capacity of a commercial Li-ion battery as a function of cycle number. The cycling temperature was held constant at 25 °C. The predicted remaining useful life (RUL) of a commercial battery was also plotted against the actual RUL. The end of life of two different commercial batteries was determined to be cycle (b) 150 and (c) 30. Even though both batteries perform differently, the model was able to model the RUL with moderate to excellent accuracy. The shaded blue regions indicate ±1 standard deviation. Data taken with permission from Zhang *et al.*, Nat. Commun. **11**(1), 1706 (2020). Copyright 2020 Springer Nature.

collected and used as training data in a Gaussian process regression model that can predict capacity and remaining useful life. The trend in the loss of capacity upon cycling was accurately modeled by training the regression model on four cells cycled at room temperature and testing it on an unknown dataset of cells cycled at the same temperature [Fig. 8(a)]. In addition, the regression model could predict the remaining useful life and end of life (the cycle number in which the capacity drops below 80% of its initial value) of two commercial batteries based solely on the EIS measurement at the current cycle. Even though the two batteries can endure a significantly different number of cycles before their end-of-life, 150 cycles [Fig. 8(b)] and 30 cycles [Fig. 8(c)], the model was still able to predict the end-of-life within ±1 standard deviation (shaded blue region).

Applying data science to reliability testing requires access to large datasets. These are necessary to provide the machine learning model with enough data to extrapolate trends, which are not obvious to humans. Unfortunately, collecting enough experimental reliability data can take months, if not years. However, there are creative ways in which this problem can be alleviated. Olivetti and co-workers explored compositional landscapes through the automated extraction of literature-reported calcium aluminosilicates to examine useful precursors for the synthesis of cementitious materials. This approach collected and classified over 23 000 materials from 7000 journal articles. These text-mined data were then used to develop a machine learning model to predict the dissolution rates of materials as a function of chemical, physical, and experimental features. Decision tree regression models also identified pH, inverse absolute temperature, and non-bridging oxygen per tetrahedron as the most essential features in predicting dissolution rate.[54] Alternatively, Sun *et al.* constructed a machine learning regression model that uses color change as a descriptor for the degradation of coated methylammonium lead iodide thin films. An image of the material was taken at different time points during aging, and the red, green, and blue color values were extracted to monitor degradation rates as a function of time. These data and additional descriptors for the potential coating materials and their processing conditions, such as the concentration of the capping layer, were used to train a machine learning model to predict the degradation onset time. Upon model optimization, the machine learning model was able to identify that the most important features of a robust capping layer are a low number of hydrogen-bonding donors and a small topological polar surface area.[55] Considering that the main evidence of K_2SiF_6:Mn^{4+} undergoing hydrolysis is a change in body color, this methodology could also be applied to body color changes observed in phosphors. However, there are no reports of using these approaches to improve our understanding of materials degradation to date, making this an outstanding research opportunity.

B. Turning to high-throughput computational modeling in the absence of experimental data

Applying data science to guide research has remained limited in many fields because large experimental datasets are not available since some properties are difficult (or expensive) to measure for many materials. An alternative approach is to use computation to model a material's response to external stimuli and use the results to train machine learning models. For example, semiconductors are used in several fields, including photovoltaics,[56] transistors,[57] and light-emitting diodes.[58] The most common method to tune a semiconductor's properties is by introducing dopants or impurities. This is similar

to rare-earth substituted phosphor chemistry. Unfortunately, even dilute concentrations of these impurities can change a material's electronic structure and act as a failure mode that shuts down physical properties. For example, a substitutional dopant in a semiconductor with energy levels inside the bandgap can reduce photovoltaic efficiency through non-radiative recombination of charge carriers or enable sub-gap absorption if the energy levels are partially filled.[59] To better understand the formation likelihood and electronic levels of point defects in binary group IV, III–V, and II–V1 cubic zinc blende semiconductors, Chan and co-workers calculated the defect formation energy as a function of charge, chemical potential, and Fermi level using density functional theory (DFT).[59] The total number of possible impurities based on the considered chemical space was approximately 12 474. Obviously, it is not feasible to calculate the defect formation energies of every possible composition. However, a training set can still be constructed by performing DFT calculations on only 10% of the entire composition space as long as every compound, element, and defect site (substitutional or interstitial) is nearly equally represented. A machine learning model can then be built to predict the neutral state formation energy and six types of charge transition levels for any possible impurity. This can allow for the rapid identification of certain impurities, which can impede the physical properties of a semiconductor. Similar ideas could be applied to phosphor development.

DFT calculations yield a static picture of the effects of external stimuli. Instead, we can turn to *ab initio* molecular dynamics (AIMD) simulations, which generate finite-temperature dynamical trajectories using forces obtained from electronic structure calculations and allow researchers to monitor chemical bonds breaking and forming over a specific time frame.[60] Within the simulations, different ensembles can be applied, such as the microcanonical (NVE) or canonical (NVT) ensembles where total energy or simulation temperature is held constant, respectively. With the current focus on reliability, these simulations can model the effects of different applied stimuli, such as water and oxygen adsorption on a phosphor surface,[61] light exposure,[62] and pressure[63] at a constant temperature. For example, the evolution of interatomic distances was monitored upon water adsorption on the (100) surface of CH_3NH_3I-terminated $CH_3NH_3PbI_3$. It was found that the Pb–I distance increases as a function of simulation time, which corresponds to the bonds breaking upon water adsorption and confirms surface degradation upon contact with moisture [Figs. 9(a) and 9(b)]. Conversely, as shown in Figs. 9(c) and 9(d), the Cs–I bond lengths on a CsI-terminated γ-$CsPbI_3$ (220) surface remain relatively unchanged by the end of the simulation time, indicating that there is no visible surface distortion caused by water adsorption.[64] This methodology can be applied to phosphors where the simulation time passed until bonds are broken (large interatomic distances), and the adsorption energy of a water molecule of a variety of phosphor surfaces can be collected to predict hydrolysis resistance. Similarly, the oxygen adsorption energies and the distances between adsorbed oxygen and the rare-earth can be used to quantify oxygen resistance in phosphors. It is also possible that the compatibility of a coating material with respect to the phosphor surface and the stability of the coating material with respect to hydrolysis and oxidation can also be modeled using AIMD simulations and the failure modes identified. Ultimately, AIMD simulations can be used to understand degradation mechanisms of a particular

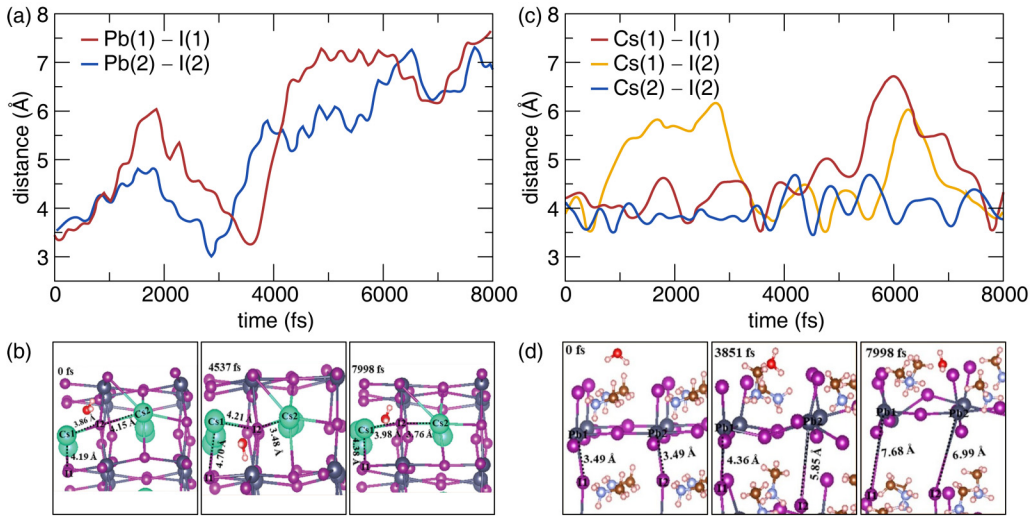

FIG. 9. (a) The distance between Pb(1)–I(1) (red) and Pb(2)–I(2) (blue) upon the surface adsorption of a water molecule over the course of 8000 fs. (b) The crystal structure of a (100) surface of CH_3NH_3I-terminated $CH_3NH_3PbI_3$ after 0 fs (left), 4537 fs (middle), and 7998 fs (right) illustrate the Pb–I bond lengths increasing to the point of bonds breaking. (c) Conversely, the bond distances between Cs(1)–I(1) (red), Cs(1)–I(2) (yellow), and Cs(2)–I(2) (blue) show a slight increase over the course of the simulation and end at distances similar to the initial distances, indicating relatively little effect on the bonds from water adsorption. (d) The crystal structure of the CsI-terminated γ-$CsPbI_3$ (220) surface shows that the Cs–I distances show little change after 0 fs (left), 3851 fs (middle), and 7998 fs (right). Reproduced with permission from Busipalli *et al.*, Phys. Chem. Chem. Phys. **22**(10), 5693–5701 (2020). Copyright 2020 Royal Society of Chemistry.

phosphor with respect to external stimuli. The collection of these data can be used to supplement experimental data and create large datasets quantifying the reliability of phosphors, which can be used as training data for machine learning.

There are additional challenges toward adapting high-throughput computational modeling toward a light-based damage mechanism. Perhaps the largest initial challenge is that light-based degradation of inorganic LED phosphors has not been extensively discussed in the open literature, unlike semiconductor quantum dots, and is often kept as proprietary corporate information. However, we give a notional mechanism for how phosphors can degrade under high-intensity blue light:

1. The population of high-energy states under high-intensity blue excitation, either through excited-state absorption or energy transfer between two excited ions. This process is similar to upconversion processes.
2. Interactions between excited ions in higher-energy states and extended host-lattice states (e.g., host-lattice conduction and valence bands) lead to a mobile charge in the valence or conduction band.
3. Trapping of the mobile charge by defects or impurities in the host lattice, as in afterglow or persistent phosphors. Charge trapping results in color centers that quench luminescence either by resonant energy transfer or electron transfer.

Assessing and quantifying each step in this process can be experimentally difficult, even for well-equipped laboratories. In addition, since typical phosphor quantum efficiencies are greater than 80% and often greater than 90%, the relative probabilities for the processes for light-induced damage are relatively low vs a radiative transition. However, each step in the notional mechanism(s) listed above is amenable to computational methods. Understanding how high-energy states are populated under blue light excitation requires insight into rare-earth electronic structures and transition probabilities in a given host, where there has been significant progress in developing phenomenological and calculation tools to understand level structure vs ion coordination and bonding.[18–24,65] Investigating interactions that can lead to a mobile charge can build upon recent work toward understanding ionization-based quenching[66] to determine the relative position of excited states within host-lattice bandgaps. Finally, trapped mobile charges could be addressed through calculations of defect formation energies and the positions of defects within host bandgaps to understand the potential for charge trapping as has been done in persistent phosphor systems.[67] There are inherent challenges to incorporating three separate calculations into a usable metric, but even an initial assessment of light-induced degradation could provide early information to researchers on potential risks and benefits in the development cycle of a new material. As a starting point, it could be useful to understand defect formation energies in known phosphor hosts with their charge trapping capability and apply that information toward the potential for light-based damage.

C. Applying machine learning to reliability testing

The data sets used to train machine learning models are often composed of compositional information (atomic number, atomic weight, group number, etc.), atomic size information (atomic radius, ionic radius, etc.), materials properties (melting point, bandgap, space group number, etc.), and electronic information (Pauling electronegativity, valence electron count, etc.).[68] Local structure information can also be included. The most essential descriptors for each of these datasets would be related to the reliability of information gathered from experiments, DFT calculations, or AIMD simulations. These data sets can then be trained using various algorithms and tested by predicting the properties of unseen data.

Machine learning has already been successfully used to identify new phosphors. For example, it has been established that a host structure's bandgap (E_g) and the Debye temperature (Θ_D) loosely correlate with a phosphor's optical properties. However, there are a few publications that report the experimentally measured Θ_D. To supplement this, the $\Theta_{D,DFT}$ of 2610 compounds, calculated by the Materials Project, served as training data to predict the Debye temperature using a support vector regression analysis ($\Theta_{D,SVR}$). The resulting machine learning model predicted the Θ_D of over 100 000 compounds extracted from Pearson's Crystal database. Plotting the $\Theta_{D,SVR}$ against the bandgap produced a sorting diagram that revealed $NaBaB_9O_{15}$:Eu^{2+} as a promising host crystal structure. The subsequent synthesis and excellent optical properties of this phosphor [QE = 95(1)% and zero thermal quenching] were attributed to these structural properties and highlight the success of using machine learning for phosphor discovery.[69] Similarly, a machine learning model was constructed to predict a material's centroid shift (ε_C) as an initial proxy for emission wavelength. This required first determining the host structure's relative permittivity, ε_r. Calculating ε_r using DFT is computationally expensive; however, it is possible to predict this property using machine learning with descriptors, including average cation electronegativity, average anion polarizability, ionic radius, and average bond length, among others [Fig. 10(a)]. The resulting support vector machine predicted $\varepsilon_{r,SVR}$ was then used as one of the descriptors to predict ε_C. The resulting model, provided in Fig. 10(b), showed excellent agreement between the experimental, $\varepsilon_{C,exp}$, and extreme gradient boosted (XGB), $\varepsilon_{C,XGB}$, machine learning values of the centroid shift. The feature importance in this model was also analyzed in Fig. 10(c) to understand the dominating factors guiding centroid shift. The average anion polarizability (α_{av}) yields the greatest improvement, or gain, to the machine learning model, making it the most important feature for predicting $\varepsilon_{C,XGB}$.[70] These findings highlight the potential of using machine learning to predict a phosphor's basic optical properties. Applying machine learning starting from DFT-based training data is clearly a viable method for accessing difficult-to-predict properties.

Most examples using computational data to feed machine learning models use DFT outputs, which may not be particularly useful for understanding a material's environmentally induced failure. AIMD simulations may be more informative, but these calculations are far more computationally expensive than routine first-principles calculations. It has been proposed that advancements in software design and parallel algorithms will be integral in making these calculations more accessible.[60] While waiting for these improvements, an active learning approach can also be

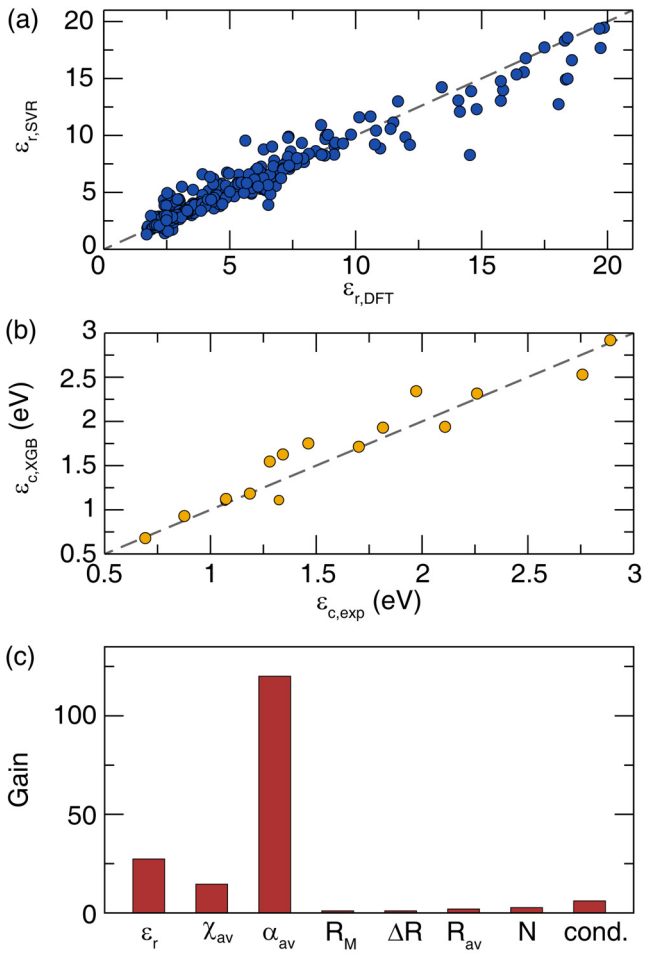

FIG. 10. (a) The DFT calculated values of relative permittivity, $\varepsilon_{r,DFT}$, vs the support vector machine learning predicted relative permittivity $\varepsilon_{r,SVR}$ for a 10% holdout test. The ideal line is shown as the dashed gray line. (b) The experimental values of the centroid shift, $\varepsilon_{C,exp}$, vs the extreme gradient boosted machine learning predicted values of the centroid shift, $\varepsilon_{C,XGB}$. The data represent 10% of the training set, and the ideal line is shown as the dashed gray line. (c) A feature importance test can be carried out in terms of gain in the model performance. It is clear that the average anion polarizability, α_{av}, is more important than relative permittivity ($\varepsilon_{r,SVR}$), average cation electronegativity (χ_{av}), ionic radius (R_M), difference in radius (ΔR), average bond length (R_{av}), coordination number (N), and condensation (cond.) in determining the centroid shift. Reproduced with permission from Zhuo *et al.*, J. Appl. Phys. **128**(1), 013104 (2020). Copyright 2020 AIP Publishing LLC.

considered.[71] A small data set collected from AIMD simulations can first be used to train a machine learning model. The areas in which the model has high uncertainty can then direct further computational investigations until the accuracy of the model has improved. Similarly, the model's predictions can be experimentally investigated, and the results can also be fed back into the model in an iterative process.

VI. CONCLUSIONS

The focus on downconverters for energy-efficient solid-state lighting and display applications has led to the identification of numerous new phosphors with excellent optical properties; however, the reliability of nearly every material reported in the literature is not discussed. A phosphor must be able to withstand degradation from high-intensity light excitation, ambient moisture, and high operating temperatures to be considered for commercial implementation since these degradation pathways can cause irreversible and unacceptable losses in lumen output or shifts in emission color. Current insights into these degradation mechanisms stem from exhaustive iterative testing, such as monitoring phosphor intensity as a function of temperature or incident light flux. Unfortunately, it is difficult to identify concrete methods to mitigate this response since different combinations of these failure modes can coincide. Alternatively, one of the most promising opportunities for understanding and preventing failure modes in phosphors is to use data-driven techniques. The data gathered from iterative testing can be used for training a machine learning model to predict the mean time to failure or the features contributing to a robust material. If experimental datasets are not available or feasible, first-principles calculations and simulations will play an essential role in modeling reliability. The recent advances in *ab initio* molecular dynamics simulations make it possible to monitor chemical bonds breaking and forming upon applied stimuli, such as adsorbed water and oxygen molecules, pressure, and light. The data collected from these computational investigations can also be used to train machine learning models to identify unforeseen trends in data. Continual improvements to software design and algorithms will be instrumental in transitioning to high-throughput reliability screening and will transform how these materials are synthesized, processed, and measured.

ACKNOWLEDGMENTS

S.H. and J.B. would like to thank the National Science Foundation (No. CER-1911311) as well as the Welch Foundation (No. E-1981) for supporting this work. A.A.S., J.E.M., S.P.S., and F.G.-S. acknowledge the U.S. Department of Energy (No. DE-EE00003251) for support of initial spectroscopic work and thank their colleagues at Current LLC (formerly GE Lighting) and GE Global Research, specifically A. I. Chowdhury, R. J. Lyons, N. P. Kumar, D. G. Porob, W. E. Cohen, F. Du, W. W. Beers, and C. Nelson, for their contributions on the development of the $K_2SiF_6:Mn^{4+}$ phosphor.

AUTHOR DECLARATIONS

Conflict of Interest

The authors have no conflicts to disclose.

Author Contributions

Shruti Hariyani: Conceptualization (equal); Data curation (equal); Formal analysis (equal); Funding acquisition (equal); Visualization (equal); Writing – original draft (equal). **Jakoah Brgoch:** Conceptualization (equal); Funding acquisition (equal);

Visualization (equal); Writing – original draft (equal). **Florencio Garcia-Santamaria:** Conceptualization (equal); Funding acquisition (equal); Investigation (equal); Methodology (equal); Validation (supporting); Writing – original draft (equal); Writing – review & editing (supporting). **Srinivas P. Sista:** Funding acquisition (equal); Investigation (supporting); Methodology (equal); Validation (supporting); Writing – review & editing (supporting). **James E. Murphy:** Funding acquisition (equal); Investigation (equal); Methodology (equal); Validation (supporting); Writing – review & editing (supporting). **Anant A. Setlur:** Conceptualization (equal); Data curation (equal); Formal analysis (equal); Funding acquisition (equal); Investigation (supporting); Validation (supporting); Writing – original draft (equal).

DATA AVAILABILITY

The data that support the findings of this study are available within the article.

REFERENCES

[1]U. S. Department of Energy *2022 Solid-State Lighting R&D Opportunities*. (accessed August 2022); available at https://www.energy.gov/sites/default/files/2022-02/2022-ssl-rd-opportunities.pdf
[2]N. Fumo and L. M. Chamra, Appl. Energy **87**, 2023 (2010).
[3]Z. Xia and Q. Liu, Prog. Mater. Sci. **84**, 59 (2016).
[4]X. Ji, J. Zhang, Y. Li, S. Liao, X. Zhang, Z. Yang, Z. Wang, Z. Qiu, W. Zhou, L. Yu, and S. Lian, Chem. Mater. **30**, 5137 (2018).
[5]K. A. Denault, N. C. George, S. R. Paden, S. Brinkley, A. A. Mikhailovsky, J. Neuefeind, S. P. DenBaars, and R. Seshadri, J. Mater. Chem. **22**, 18204 (2012).
[6]S. Takemura, Y. Koyama, T. Nakanishi, S. Funahashi, N. Hirosaki, H. Ikeno, and T. Takeda, Scr. Mater. **215**, 114686 (2022).
[7]X. Huang, Sci. China Mater. **63**, 325 (2020).
[8]U. S. Department of Energy *Hammer Testing Findings for Solid-State Lighting Luminaires*. (accessed August 2022); available at https://www1.eere.energy.gov/buildings/publications/pdfs/ssl/hammertest_reportsummary_jan2014.pdf
[9]M.-H. Chang, D. Das, P. V. Varde, and M. Pecht, Microelectron. Reliab. **52**, 762 (2012).
[10]W. D. Van Driel, B. Jacobs, P. Watte, and X. Zhao, Microelectron. Reliab. **129**, 114477 (2022).
[11]P. Pust, P. J. Schmidt, and W. Schnick, Nat. Mater. **14**, 454 (2015).
[12]U. S. Department of Energy, Yuma Border Patrol Area Lighting Retrofit. **2018**, (accessed August 2022); available at https://www.energy.gov/sites/default/files/2018/05/f51/SSL_Yuma_Final%20LED%20System%20Performance%20Assessment_0.pdf
[13]P. F. Smet, A. B. Parmentier, and D. Poelman, J. Electrochem. Soc. **158**, R37 (2011).
[14]J. L. Leaño, M.-H. Fang, and R.-S. Liu, ECS J. Solid State Sci. Technol. **7**, R3111 (2018).
[15]S. Li and R.-J. Xie, ECS J. Solid State Sci. Technol. **9**, 016013 (2020).
[16]Y.-C. Lin, M. Karlsson, and M. Bettinelli, in *Photoluminescent Materials and Electroluminescent Devices* (Springer, 2017), p. 309.
[17]R.-J. Xie and N. Hirosaki, Sci. Technol. Adv. Mater. **8**, 588 (2007).
[18]P. Dorenbos, Phys. Rev. B **62**, 15640 (2000).
[19]P. Dorenbos, Phys. Rev. B **62**, 15650 (2000).
[20]P. Dorenbos, Phys. Rev. B **64**, 125117 (2001).
[21]P. Dorenbos, J. Alloys Compd. **341**, 156 (2002).
[22]P. Dorenbos, Phys. Rev. B **65**, 235110 (2002).
[23]P. Dorenbos, J. Lumin. **99**, 283 (2002).
[24]P. Dorenbos, J. Lumin. **135**, 93 (2013).
[25]J. M. Phillips, M. E. Coltrin, M. H. Crawford, A. J. Fischer, M. R. Krames, R. Mueller-Mach, G. O. Mueller, Y. Ohno, L. E. S. Rohwer, J. A. Simmons, and J. Y. Tsao, Laser Photonics Rev. **1**, 307 (2007).
[26]International Electrotechnical Commission, Lamps, Light Sources and LED Packages for Road Vehicles - Performance Requirements. IEC 60810:2017 Apr. 2022. Available at https://webstore.iec.ch/publication/75728
[27]SAE International Surface Vehicle Recommended Practice, Test Methods and Equipment for Lighting Devices and Components for Use on Vehicles Less than 2032 mm in Overall Width. SAE Standard J575: Nov. 2006. Available at https://www.sae.org/standards/content/j575_202104/
[28]T. Isobe, ECS J. Solid State Sci. Technol. **2**, R3012 (2013).
[29]C.-W. Yeh, W.-T. Chen, R.-S. Liu, S.-F. Hu, H.-S. Sheu, J.-M. Chen, and H. T. Hintzen, J. Am. Chem. Soc. **134**(34), 14108 (2012).
[30]C.-Y. Wang, R.-J. Xie, F. Li, and X. Xu, J. Mater. Chem. C **2**, 2735 (2014).
[31]S. Oshio, J. Electrochem. Soc. **145**, 3903 (1998).
[32]P. F. Smet, I. Moreels, Z. Hens, and D. Poelman, Materials **3**, 2834 (2010).
[33]Y. Zhao, L. Yin, O. M. Ten Kate, B. Dierre, R. Abellon, R.-J. Xie, J. R. Van Ommen, and H. T. Hintzen, J. Mater. Chem. C **7**, 5772 (2019).
[34]R. J. Lyons, A. A. Setlur, A. R. Deshpande, and L. S. Grigorov, "Color stable manganese-doped phosphors," U.S. patent 8,252,613 (28 August 2012).
[35]A. A. Setlur, O. P. Siclovan, R. J. Lyons, and L. S. Grigorov, "Moisture-resistant phosphor and associated method," U.S. patent 8,057,706 (15 November 2011).
[36]R. Verstraete, H. F. Sijbom, J. J. Joos, K. Korthout, D. Poelman, C. Detavernier, and P. F. Smet, ACS Appl. Mater. Interfaces **10**, 18845 (2018).
[37]Y. Zhao, Q. Guan, H. Wang, Y. Li, J. Lu, and R.-J. Xie, J. Mater. Chem. C **10**, 9867 (2022).
[38]J. E. Murphy and F. Garcia, "Coated manganese doped phosphors," U.S. patent 11,008,509 (18 May 2021).
[39]S. Hariyani and J. Brgoch, ACS Appl. Mater. Interfaces **13**, 16669 (2021).
[40]Y. Zhuo, S. Hariyani, J. Zhong, and J. Brgoch, Chem. Mater. **33**, 3304 (2021).
[41]A. A. Setlur, J. J. Shiang, and U. Happek, Appl. Phys. Lett. **92**, 081104 (2008).
[42]M. A. Van de Haar, M. Tachikirt, A. C. Berends, M. R. Krames, A. Meijerink, and F. T. Rabouw, ACS Photonics **8**, 1784 (2021).
[43]N. J. Orfield, S. Majumder, Z. Hu, F. Y.-C. Koh, H. Htoon, and J. A. Hollingsworth, ACS Appl. Mater. Interfaces **12**, 30695 (2020).
[44]F. Yao, L. Wang, Y. Lv, Y. Zhuang, T.-L. Zhou, and R.-J. Xie, J. Mater. Chem. C **6**, 890 (2018).
[45]M. A. Shah, D. G. Lee, B. Y. Lee, and S. Hur, IEEE Access **9**, 140079 (2021).
[46]A. A. Setlur, J. E. Murphy, and S. P. Sista, ECS J. Solid State Sci. Technol. **9**, 016018 (2020).
[47]X.-D. Sun, C. Gao, J. Wang, and X.-D. Xiang, Appl. Phys. Lett. **70**, 3353 (1997).
[48]R. A. Potyrailo, K. Ezbiansky, B. J. Chisholm, W. G. Morris, J. N. Cawse, L. Hassib, G. Medford, and H. Reitz, J. Comb. Chem. **7**, 190 (2005).
[49]J. E. Murphy, A. A. Setlur, F. Garcia, R. J. Lyons, A. I. Chowdhury, N. Karkada, and P. K. Nammalwar, "Color stable red-emitting phosphors," U.S. patent 8,906,724 (9 December 2014).
[50]J. E. Murphy, A. A. Setlur, F. Garcia, R. J. Lyons, A. I. Chowdhury, N. Karkada, and P. K. Nammalwar, "Color stable red-emitting phosphors," U.S. patent 9,580,648 (28 February 2017).
[51]S. Saxena, Y. Xing, and M. G. Pecht, *Prognostics and Health Management of Electronics: Fundamentals, Machine Learning, and the Internet of Things* (Springer, 2020).
[52]Y. Zhang, Q. Tang, Y. Zhang, J. Wang, U. Stimming, and A. A. Lee, Nat. Commun. **11**(1), 1706 (2020).
[53]N. A. Canas, K. Hirose, B. Pascucci, N. Wagner, K. A. Friedrich, and R. Hiesgen, Electrochim. Acta **97**, 42 (2013).
[54]H. Uvegi, Z. Jensen, T. N. Hoang, B. Traynor, T. Aytaş, R. T. Goodwin, and E. A. Olivetti, J. Am. Ceram. Soc. **104**, 3042 (2021).

[55]N. T. P. Hartono, J. Thapa, A. Tiihonen, F. Oviedo, C. Batali, J. J. Yoo, Z. Liu, R. Li, D. F. Marrón, M. G. Bawendi, T. Buonassisi, and S. Sun, Nat. Comm. **11** (1), 4172 (2020).
[56]R. W. Miles, G. Zoppi, and I. Forbes, Mater. Today **10**, 20 (2007).
[57]E. Fortunato, P. Barquinha, and R. Martins, Adv. Mater. **24**, 2945 (2012).
[58]A. Ren, H. Wang, W. Zhang, J. Wu, Z. Wang, R. V. Penty, and I. H. White, Nat. Electron. **4**, 559 (2021).
[59]A. Mannodi-Kanakkithodi, X. Xiang, L. Jacoby, R. Biegaj, S. T. Dunham, D. R. Gamelin, and M. K. Y. Chan, Patterns **3**, 100450 (2022).
[60]R. Iftimie, P. Minary, and M. E. Tuckerman, Proc. Natl. Acad. Sci. U.S.A. **102**, 6654 (2005).
[61]J. Wu, J.-H. Li, and Y.-X. Yu, ChemPhysChem **21**, 2539 (2020).
[62]Y. Ouyang, Y. Li, P. Zhu, Q. Li, Y. Gao, J. Tong, L. Shi, Q. Zhou, C. Ling, Q. Chen, Z. Deng, H. Tan, W. Deng, and J. Wang, J. Mater. Chem. A **7**, 2275 (2019).
[63]L. Koči, R. Ahuja, L. Vitos, and U. Pinsook, Phys. Rev. B **77**, 132101 (2008).
[64]D. L. Busipalli, K.-Y. Lin, S. Nachimuthu, and J.-C. Jiang, Phys. Chem. Chem. Phys. **22**(10), 5693 (2020).
[65]J. Wen, L. Ning, C.-K. Duan, Y. Chen, Y. Zhang, and M. Yin, J. Phys. Chem. C **116**, 20513 (2012).
[66]M. Amachraa, Z. Wang, C. Chen, S. Hariyani, H. Tang, J. Brgoch, and S. P. Ong, Chem. Mater. **32**, 6256 (2020).
[67]E. Finley, A. Mansouri Tehrani, and J. Brgoch, J. Phys. Chem. C **122**, 16309 (2018).
[68]G. G. C. Peterson and J. Brgoch, J. Phys. Energy **3**, 022002 (2021).
[69]Y. Zhuo, A. Mansouri Tehrani, A. O. Oliynyk, A. C. Duke, and J. Brgoch, Nat. Commun. **9**, 4377 (2018).
[70]Y. Zhuo, S. Hariyani, S. You, P. Dorenbos, and J. Brgoch, J. Appl. Phys. **128**(1), 013104 (2020).
[71]S. J. Ang, W. Wang, D. Schwalbe-Koda, S. Axelrod, and R. Gómez-Bombarelli, Chem **7**, 738 (2021).